Effect of the Difference in Strength of Hard and Soft Components on the Synergetic Strengthening of Layered Materials

Jung Gi Kim[1] · Jae Wung Bae[2] · Jeong Min Park[2] · Wanchuck Woo[3] · Stefanus Harjo[4] · Sunghak Lee[2] ·
Hyoung Seop Kim[2,5]

Abstracts

Heterogeneous structured materials achieve a combination of high strength and extreme ductility due to synergetic strengthening driven by conditions in the interfacial region. Although the origin of synergetic strengthening has been revealed to be strain incompatibility in the interfacial region, the effect of the strength difference between hard and soft phases on strengthening has not been investigated well. In the work reported in the present paper, the effect of the difference in strength of the hard and soft phases on synergetic strengthening was investigated by conducting in situ neutron diffraction tensile tests. As a result, it was determined that the dislocation density in a layered sheet of high Mn (HMn) steel/interstitial free (IF) steel is higher than that in a layered sheet of HMn/low carbon steel. The big difference in mechanical properties between HMn steel and IF steel induces a high stress gradient and results in additional dislocations. Because of the high dislocation density and large differences in mechanical property and anisotropy in the HMn/IF layered steel sheet, upper-bound rule-of-mixtures behavior occurs. Therefore, a great difference in the mechanical properties of hard and soft components increases the synergetic strengthening of heterogeneously structured materials.

Keywords Heterostructured material · Layered structures · Neutron diffraction · Tensile test · Synergetic strengthening

1 Introduction

To achieve the combination of outstanding strength and ductility, various heterogeneously structured (HetS) materials (e.g., bimodal [1], laminated [2], gradient [3], and harmonic [4] structures) have been designed. Many studies have revealed that the improved mechanical property of HetS materials is not only related to conventional strengthening mechanisms, but is also linked with synergetic strengthening in the interfacial region [5, 6]. Synergetic strengthening of HetS materials originates from the different mechanical properties of hard and soft components, which creates incompatibility in the plastic strains that occur during plastic deformation [7]. To maintain strain continuity during plastic deformation, the accumulation of geometrically necessary dislocations (GNDs) occurs in the interfacial region and these accumulated GNDs contribute to synergetic strengthening of HetS materials.

Because synergetic strengthening enhances the strength and ductility of HetS materials, the quantification of synergetic strengthening is an important issue for maximizing their mechanical properties. In previous studies, synergetic strengthening was quantified in a variety of ways. These included measuring the GND pile-up using electron backscatter diffraction (EBSD) analysis [8, 9], dislocation density with in situ neutron diffraction test [10], back-stress evolution using the loading–unloading-reloading (LUR) test [11, 12], and microhardness differences [13]. These results indicate that both the

✉ Hyoung Seop Kim
hskim@postech.ac.kr

1 Department of Metallurgical and Materials Engineering, Gyeongsang National University, Jinju 52828, Republic of Korea

2 Department of Materials Science and Engineering, Pohang University of Science and Technology (POSTECH), Pohang 37673, Republic of Korea

3 Neutron Science Centre, Korea Atomic Energy Research Institute (KAERI), Daejeon 34057, South Korea

4 J-PARC Center, Japan Atomic Energy Agency, Tokai, Ibaraki 319-1195, Japan

5 Center for High Entropy Alloys, Pohang University of Science and Technology (POSTECH), Pohang 37673, Republic of Korea

strength and dislocation density of HetS materials are higher than those of monolithic components, and that the amount of synergetic strengthening depends on the mechanical property of the hard and soft components.

Theoretically, the magnitude of a stress gradient increases as the difference in strength increases between the hard and soft components [14]. Because the accumulated dislocation density is related to the steepness of the stress gradient, the synergetic strengthening of HetS materials can be controlled by selecting hard and soft parent materials. For example, Wang et al. report that the back-stress of Cu/Cu30Zn/Cu layered material is larger than that of Cu/Cu10Zn/Cu layered material due to the large difference in mechanical properties of the Cu-sheath and Cu30Zn-core [15]. This strength difference between hard and soft components makes a steep hardness gradient at the interface. From these results, we would expect that a large strength difference between hard and soft components would not only induce high back-stress from the strong coupling process, but would also provide high GND accumulation in the interfacial region. Previous research explained well the differences in back-stress evolution of the layered materials depending on the differences in mechanical properties of each constituent. However, quantification of accumulated dislocations in HetS materials has not yet been performed.

In this study, the effect of the difference in mechanical properties of hard and soft components on the synergetic strengthening of HetS materials was investigated by quantifying the dislocation density. Evolution of the dislocation density during plastic deformation was estimated using an in situ neutron diffraction tensile test by measuring the diffraction peaks of deformed layered steels. From the neutron diffraction peaks, both lattice strain (ε_{hkl}) and dislocation density were quantified by conducting diffraction peak profile analysis.

2 Experimental Procedure

The chemical compositions of high Mn (HMn), low carbon (LC), and interstitial free (IF) steels are represented in Table 1. Table 2 represents the stacking ratio of the layered steel sheets. Each layered steel sheet was fabricated by conducting a roll-bonding process. For example, in the case of a 1 (mild steel): 2 (HMn steel): 1 (mild steel) stacking ratio of a layered steel sheet, a 20 mm-thick HMn (core) steel and 10 mm-thick LC or IF (sheath) steel plates were bonded by welding along the edges (sides) of plates. The stacked steel sheets were homogenized at 1200 °C for 1 h and hot rolled from 40 to 2.5 mm

Table 1 Chemical composition of HMn, LC, and IF steels

wt%	C	Mn	Al
HMn	0.6	15	1.2
LC	0.03	0.2	0.04
IF	0.002	0.2	0.04

Table 2 Stacking ratio of the layered steel sheets

	LC/IF	HMn	LC/IF
161	0.125	0.75	0.125
121	0.25	0.5	0.25
111	0.33	0.33	0.33

thickness at 900–1100 °C. After the hot rolling process, the sheets were cold rolled from 2.5 to 1 mm thickness and annealed at 820 °C for 30 s. Briefly, the HMn/LC layered steel is labeled LC/HMn/LC while the HMn/IF layered steel is labeled IF/HMn/IF. Figure 1 represents the phase maps of the layered steel sheets with electron backscatter diffraction (EBSD; Hikari, EDAX, USA) analyses. Both LC/HMn/LC and IF/HMn/IF have distinguished interfaces while there are no significant defects at the interface as reported in the previous studies [16, 17].

The mechanical property of layered steel sheets was investigated by conducting room-temperature uniaxial tensile tests. Tensile specimens were prepared with a 5 mm gauge-length plate-type specimen and the tests were done using a universal testing machine (Instron 1361, Instron Corp., Canton, MA, USA) at a 1×10^{-3} s^{-1} quasi-static strain rate. To measure accurately the strain of sub-sized tensile specimens, the digital image correlation (DIC: ARAMIS v6.1, GOM Optical Measuring Techniques, Germany) method was employed using a white and black speckle pattern on the tensile specimens.

To calculate ε_{hkl} and the dislocation density evolution of the layered steel sheet, in situ neutron diffraction tensile tests were conducted. The neutron diffraction test was performed using the engineering materials diffractometer (BL-19, TAKUMI) in the Materials and Life Science Experimental Facility (MLF) of the Japan Proton Accelerator Research Complex (J-PARC) [18]. The monochromatic neutron beam ($\lambda = 0.35$ nm), high-resolution diffractometer ($\Delta d/d_{hkl} = 0.2\%$), and 5 mm radial collimator were utilized to evaluate the peak broadening during the tensile test. The in situ tensile tests were conducted at room temperature with a 1×10^{-3} s^{-1} quasi-static strain rate. To get reliable diffraction data, diffraction peaks were measured for more than 20 min at each 50 MPa spacing of an elastic deformation region and at each 5% elongation spacing for a plastic deformation region.

Figure 2 represents the neutron diffraction peaks of the IF/HMn/IF and LC/HMn/LC layered steel sheets. The peak position and full-width-at-half-maximum (FWHM) of the diffraction peaks were fitted using Z-Rietveld software [19]. To calibrate the instrumental effect, the diffraction pattern of LaB$_6$ as the standard reference material (Line shape SRM 660c, NIST, USA) was measured and implemented during peak profile analysis. The ε_{hkl} of layered materials can be calculated from a diffraction peak shift [20, 21]:
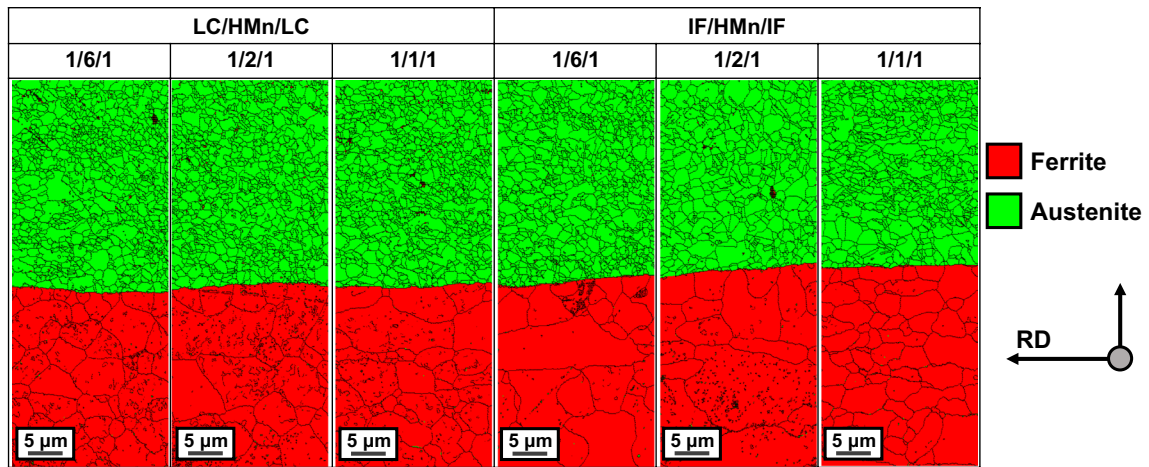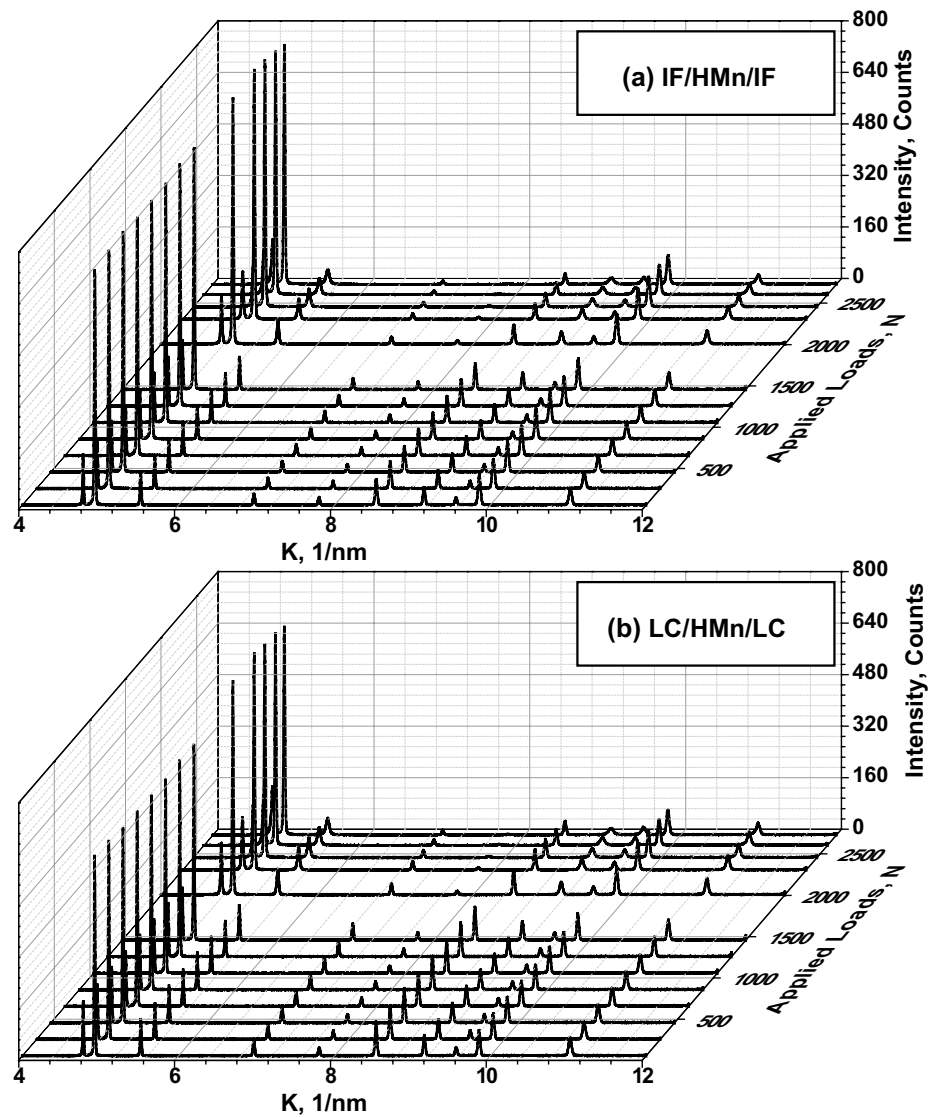
Fig. 1 Phase map at the interface of layered steel sheet

Fig. 2 Neutron diffraction patterns of the **a** IF/HMn/IF and **b** LC/HMn/LC layered steel sheets

$$\varepsilon_{hkl} = \frac{d_{hkl} - d_{hkl}^0}{d_{hkl}^0}, \tag{1}$$

where d_{hkl} is the lattice spacing of the tensile deformed specimen and d_{hkl}^0 is the lattice spacing of a specimen in an undeformed state. The dislocation density of materials can be obtained from the broadening of peak profiles using the modified Williamson–Hall plot [22]:

$$\Delta K = \frac{0.9}{D} + \left(\frac{\pi A^2 b^2}{2} \right)^{\frac{1}{2}} \rho^{\frac{1}{2}} \left(K C^{\frac{1}{2}} \right) + O\left(K^2 C \right), \tag{2}$$

where ΔK is $2 \cos \theta (\Delta\theta)/\lambda$ (FWHM), K is $2 \sin \theta/\lambda$ (peak position), θ is the diffraction angle, λ is the wavelength, A is the constant determined by the effective outer cut-off radius of dislocations, and b is the Burgers vector. In this research, the b values of HMn and LC steels were 0.2553 nm and 0.248 nm, respectively, and C is the contrast factor.

Equation (2) implies that $KC^{1/2}$ is an appropriate scaling factor for the FWHM if dislocation is the main strain factor. From the modified Williamson–Hall plot, a ΔK-$KC^{1/2}$ slope (m) can be obtained that is related to the dislocation density (ρ) of the materials [20]:

$$\rho = \frac{2}{\pi A^2 b^2} m^2. \tag{3}$$

3 Results and Discussion

Figure 3 represents the stress–strain curves of layered steel sheets and monolithic steel sheets. Although the strength of monolithic LC steel is greater than that of monolithic IF steel, the strength of LC/HMn/LC is similar to the strength of IF/HMn/IF. Moreover, the strength of IF/HMn/IF is greater than the strength estimated from the rule-of-mixtures, as shown in Fig. 4. In contrast, the strength of LC/HMn/LC is close to the strength estimated from the rule-of-mixtures [23]. This upper-bound rule-of-mixtures implies that additional strengthening occurs in the interfacial region of the layered steel sheets. Previous reports revealed that an extreme stress gradient occurs in the interfacial region and that the stress gradient increases the yield strength of materials due to the increased shear stress, which acts as an additional energy barrier to slip [24]. Because the stress gradient at the interfacial region is proportional to the strength difference between the core and sheath parts, IF/HMn/IF has a steeper stress gradient than that of LC/HMn/LC. Therefore, a large energy barrier to slip at the interface of IF/HMn/IF results in the accumulation of dislocations and the overall dislocation density of the layered steel sheet will be greater than that of monolithic steels. Such a large dislocation density in a layered steel sheet improves the macroscopic yield strength. Meanwhile, the stress gradient of LC/HMn/LC is less extreme than that of IF/HMn/IF due to the low difference in strength between the HMn steel-core and LC steel-sheath.

Fig. 3 Stress-strain curves of the IF/HMn/IF, LC/HMn/LC and monolithic steels from the conventional tensile test
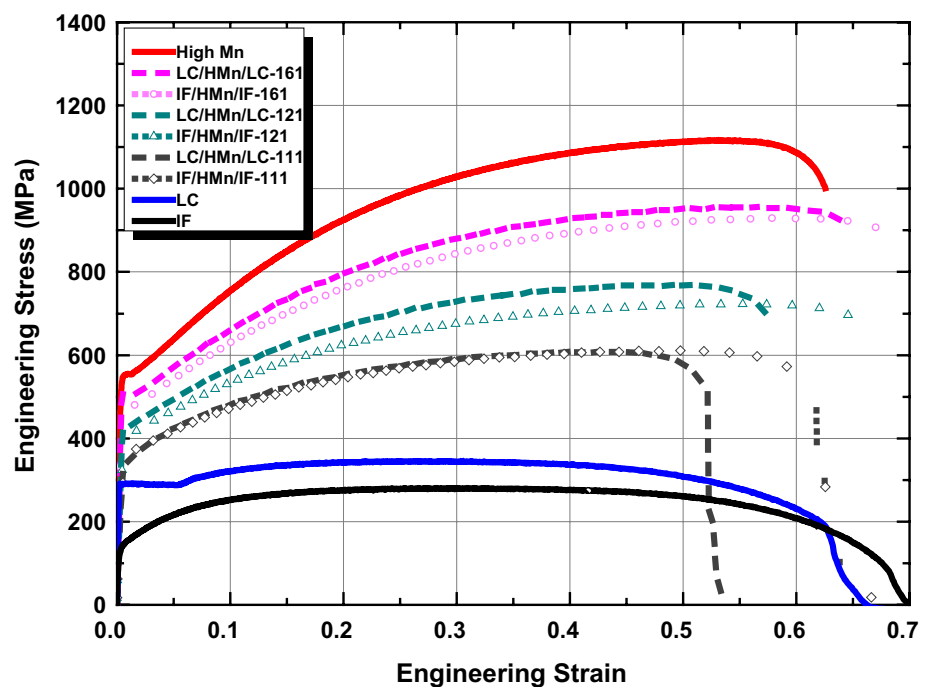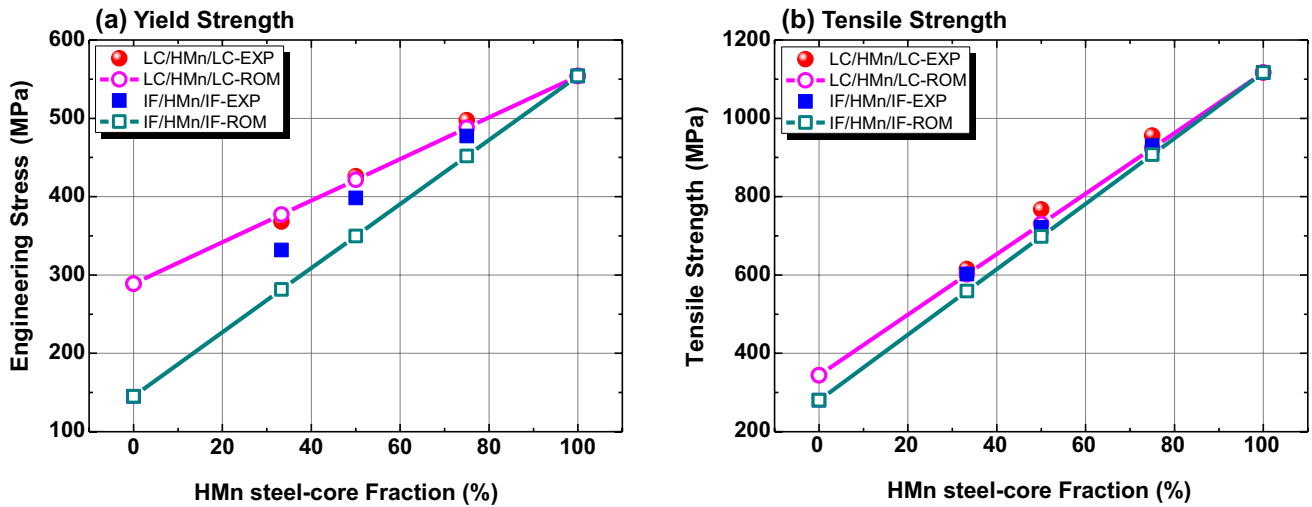
Fig. 4 The **a** yield strength and **b** tensile strength of LC/HMn/LC and IF/HMn/IF layered steel sheets compare with the estimated value by simple rule-of-mixtures

Because the amount of dislocations accumulated is proportional to the stress gradient, the added stress enhancement in LC/HMn/LC is smaller than that of IF/HMn/IF. In the later deformation stage, however, the upper-bound rule-of-mixtures tendency becomes weaker than that in the early deformation stage. The previous studies show that synergetic strengthening is effective from the early deformation stage and the amount of synergetic strengthening stays during plastic deformation [12, 25]. This means that the contribution from synergetic strengthening decreases as a plastic deformation increases. Therefore, the tensile strength of the layered steel sheet in Fig. 4b is closed to the rule-of-mixtures though the synergetic strengthening contributes to the strength enhancement.

To reveal the different evolutions of dislocation density in IF/HMn/IF and LC/HMn/LC, their deformation behaviors were investigated by conducting in situ neutron diffraction tensile tests. Figure 5a and b presents the ε_{hkl} of HMn steel-core and LC steel-sheath, respectively, as the applied load increases. As with the previous in situ neutron diffraction tensile test results for layered steel sheets, three-step ε_{hkl} partitioning occurs due to the strength difference between the HMn steel-core and LC steel-sheath [26]. In Stage 1, both the HMn steel-core and LC steel-sheath are under elastic deformation. In Stage 2, the LC steel-sheath starts plastic deformation while the HMn steel-core is still under elastic deformation. In Stage 3, both the HMn steel-core and LC steel-sheath are under plastic deformation. Because the
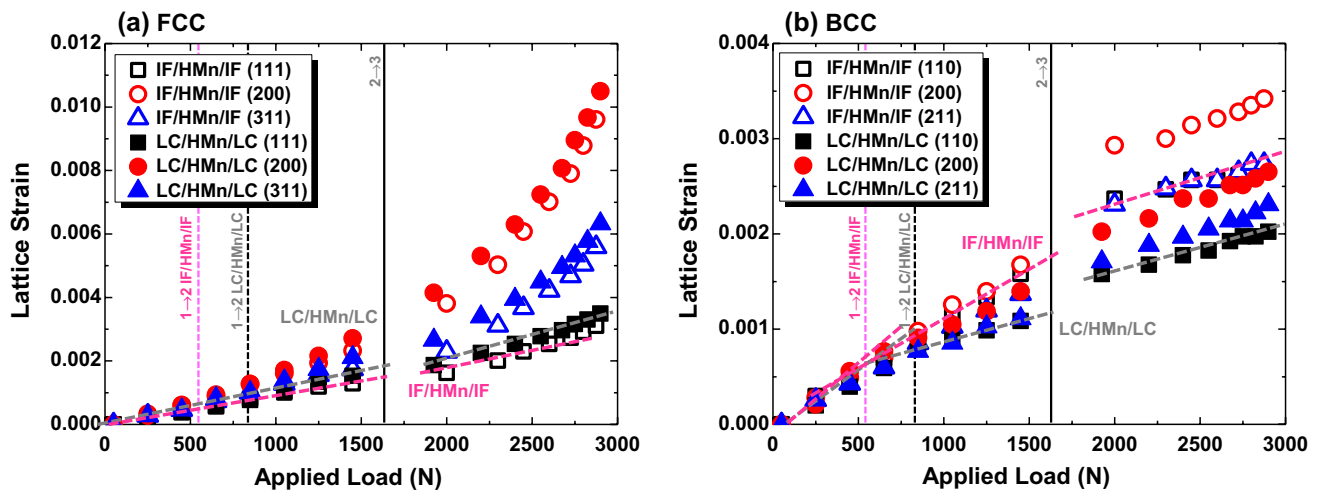

Fig. 5 The **a** FCC and **b** BCC ε_{hkl} changes of the IF/HMn/IF and LC/HMn/LC layered steel sheets

yield strength of LC steel is greater than the yield strength of IF steel, the Stage 1→2 transition of LC/HMn/LC occurs later than does that of IF/HMn/IF. The load-control→displacement-control change in mode at the Stage 2→3 transition, induces changes in the plastic strain rate, which can be proven by the ε_{hkl} jump at Stage 2→3 in Fig. 5b. The ε_{hkl} partitioning between HMn steel-core and mild steel-sheath provides plastic strain incompatibility at the interface of layered steels, and extra-GNDs will be generated to relieve this plastic-strain incompatibility. To quantify the dislocation density of layered steel sheets, m was fitted using the modified Williamson–Hall plot.

Figure 6a and b represent the modified Williamson–Hall plots of HMn steel-core and mild steel-sheath, respectively. Because the FWHM of diffraction peaks increases as the amount of plastic strain increases, the modified

Williamson–Hall plot slope m increases. In the case of the HMn steel-core, however, the m was not linearly fitted due to the existence of a stacking fault in the deformed microstructure [27]. Apart from this deviation, the m of IF/HMn/IF is always higher than that of LC/HMn/LC in both HMn steel-core and mild steel-sheath parts. Figure 7a represents changes in the m of layered and monolithic steels, calculated using the modified Williamson–Hall plots in Fig. 5. Because the dislocation density of a material is correlated with m, the dislocation density of layered materials can be plotted as shown in Fig. 7b. Because the dislocation density has a proportional relation with m, the dislocation density of IF/HMn/IF is slightly higher than that of LC/HMn/LC. However, the amount of extra-dislocation density in IF/HMn/IF is not significantly larger than that in LC/HMn/LC. This means that strengthening from extra-dislocation density is not sufficient
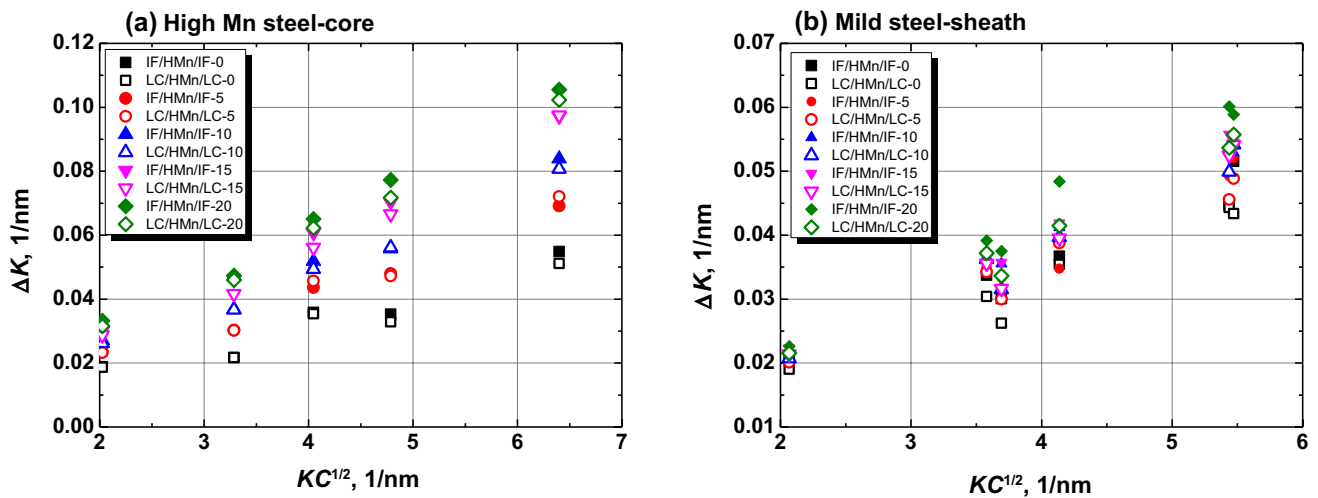

Fig. 6 Modified Williamson–Hall Plots of the **a** HMn steel-core and **b** mild steel-sheath parts in the layered steel sheets

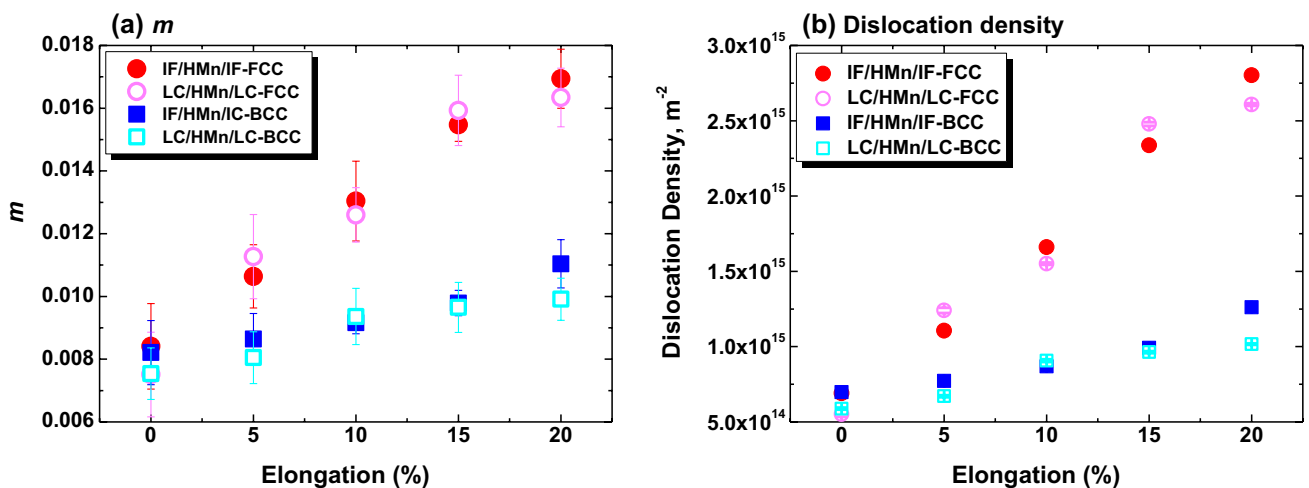**Fig. 7** **a** m and **b** dislocation density changes of the IF/HMn/IF and LC/HMn/LC layered steel sheets

to explain the large upper-bound rule-of-mixtures behavior of the IF/HMn/IF and additional explanations are required to support this result. In the previous study, the authors revealed that the differences in anisotropy and mechanical property induce tri-axial stress states at the interface of layered steel sheets [28]. Because the IF steel-sheath represents a larger strength difference with HMn steel-core than that of the LC steel-sheath, strong tri-axial stress states occur at the interface of IF/HMn/IF. Such stress states provide an additional strength to layered steel sheet during tensile test and result in the upper-bound rule-of-mixtures behavior of HetS materials [5].

Although the neutron diffraction analysis technique has limits for quantifying the accumulation of dislocations in the interfacial region, the present result indicates that the dislocation density of bulk constituents could be changed due to interfacial strengthening. Based on the in situ neutron diffraction tensile test, the difference in dislocation density between IF/HMn/IF and LC/HMn/LC could be explained by the stress gradient theory. The increased dislocation density in the HMn steel-core of IF/HMn/IF, originated from the strength difference between HMn steel-core and IF steel-sheath. As reported in the previous study, the magnitude of a stress gradient depends on the local deformation field and the stress gradient increases with the heterogeneity [15]. Because the strength difference between the HMn steel-core and IF steel-sheath is greater than that between HMn steel-core and LC steel-sheath, the amount of accumulated dislocations in the IF/HMn/IF is larger than that in the LC/HMn/LC. In contrast, the small stress gradient of LC/HMn/LC results in the limited accumulation of dislocations in the interfacial region and its dislocation density is not significantly increased. This result proves that the difference in mechanical properties of the hard and soft phases is a factor important in determining the strength that results from a synergetic strengthening of HetS materials.

4 Conclusions

In summary, the dislocation density of IF/HMn/IF and LC/HMn/LC were quantified by conducting in situ neutron diffraction tensile tests. Because of the accumulation of dislocations due to plastic strain incompatibility at the interface, the dislocation density of layered steel sheet is higher than that of monolithic steels. Moreover, the accumulated dislocation density of layered steel depends on the difference in strength of the HMn steel-core and the mild steel-sheath. Because the dislocation density of IF/HMn/IF is slight higher than that of LC/HMn/LC and large anisotropy and mechanical property differences between HMn steel-core and IF steel-sheath, the strength of IF/HMn/IF is greater than the strength estimated by the rule-of-mixtures while

the strength of LC/HMn/LC is close to that estimated using the rule-of-mixtures. Therefore, an extreme difference in mechanical properties of the hard and soft phases provides strong synergetic strengthening of HetS materials.

References

1. Q. Zhang, Y. Liu, Y. Liu, Y. Len, Y. Wu, Z. Gao, X. Wu, P. Han, Mater. Sci. Eng. A **701**, 196 (2017)
2. W.X. Yu, B.X. Liu, J.N. He, C.X. Chen, W. Fang, F.X. Yin, Mater. Sci. Eng. **767**, 138426 (2019)
3. E. Maleki, O. Unal, K.R. Kashyzadeh, Met. Mater. Int. **25**, 1436 (2019)
4. S.K. Vajpai, M. Ota, Z. Zhang, K. Ameyama, Mater. Res. Lett. **4**, 191 (2016)
5. X.L. Wu, P. Jiang, L. Chen, J.F. Zhang, F.P. Yuan, Y.T. Zhu, Mater. Res. Lett. **2**, 185 (2014)
6. E. Ma, T. Zhu, Mater. Today **20**, 323 (2017)
7. M. Yang, Y. Pan, F. Yuan, Y. Zhu, X. Wu, Mater. Res. Lett. **4**, 145 (2016)
8. X. Ma, C. Huang, J. Moering, M. Ruppert, H.W. Höffel, M. Göken, J. Narayan, Y. Zhu, Acta Mater. **116**, 43 (2016)
9. X. Wu, P. Jiang, L. Chen, F. Yuan, Y.T. Zhu, Proc. Natl. Acad. Sci. U.S.A. **111**, 7197 (2014)
10. J.G. Kim, J.W. Bae, J.M. Park, W. Woo, S. Harjo, K.-G. Chin, S. Lee, H.S. Kim, Sci. Rep. **9**, 6829 (2019)
11. X. Wu, M. Yang, F. Yuan, G. Wu, Y. Wei, X. Huang, Y. Zhu, Proc. Natl. Acad. Soc. USA **112**, 14501 (2015)
12. J.G. Kim, M.J. Jang, H.K. Park, K.-G. Chin, S. Lee, H.S. Kim, Met. Mater. Int. **25**, 912 (2019)
13. W.F. Wang, C.X. Huang, M.S. Wang, Y.S. Li, Y.T. Zhu, Scr. Mater. **150**, 22 (2018)
14. N.A. Fleck, G.M. Muller, M.F. Ashby, J.W. Hutchinson, Acta Metall. Mater. **42**, 475 (1994)
15. Y. Wang, M. Yang, X. Ma, M. Wang, K. Yin, A. Huang, C. Huang, Mater. Sci. Eng. A **727**, 113 (2018)
16. J. Park, M. Kang, S.S. Sohn, J.S. Kim, H.S. Kim, W.T. Cho, S. Lee, Mater. Sci. Eng. A **686**, 160 (2017)
17. J. Park, J.S. Kim, M. Kang, S.S. Sohn, W.T. Cho, H.S. Kim, S. Lee, Sci. Rep. **7**, 40231 (2017)
18. J. Abe, T. Hattori, K. Komatsu, H. Arima, M. Arakawa, A. Sano, H. Kagi, S. Harjo, T. Ito, A. Moriai, K. Aizawa, M. Arai, W. Utsumi, J. Phys: Conf. Ser. **215**, 012023 (2010)
19. R. Oishi-Tomiyasu, M. Yonemura, T. Morishima, A. Hoshikawa, S. Torii, T. Ishigaki, T. Kamiyama, J. Appl. Cryst. **45**, 299 (2012)
20. Y. Tomota, P. Lukas, S. Harjo, J.-H. Park, N. Tsuchida, D. Neov, Acta Mater. **51**, 819 (2003)
21. E. Gadalińska, A. Baczmański, S. Wroński, P. Kot, M. Wroński, M. Wróbel, C. Scheffzük, G. Bokuchava, K. Wierzbanowski, Met. Mater. Int. **25**, 657 (2019)
22. T. Ungár, A. Borbély, Appl. Phys. Lett. **69**, 3173 (1996)
23. S.L. Semiatin, H.R. Piehler, Metall. Trans. A **10**, 85 (1979)
24. S.S. Chakravarthy, W.A. Curtin, Proc. Nat. Aca. Soc. USA **108**, 15716 (2011)
25. C.W. Sinclair, W.J. Poole, Y. Brechet, Scr. Mater. **55**, 739 (2006)

26. M. Ojima, J. Inoue, S. Nambu, P. Xu, K. Akita, H. Suzuki, T. Koseki, Scr. Mater. **66**, 139 (2012)
27. S. Brandstetter, P.M. Derlet, S. Van Petegem, H. Van Swygen-hoven, Acta Mater. **56**, 165 (2008)
28. J.G. Kim, S.M. Baek, H.H. Lee, K.-G. Chin, S. Lee, H.S. Kim, Acta Mater. **147**, 304 (2018)